

Spin Asymmetries in Low-Energy Electron Scattering from Cesium Atoms

G. Baum, W. Raith, B. Roth, and M. Tondera

Fakultät für Physik, Universität Bielefeld, D-33615 Bielefeld, Germany

K. Bartschat

Department of Physics and Astronomy, Drake University, Des Moines, Iowa 50311

I. Bray

Electronic Structure of Materials Centre, The Flinders University of South Australia, Adelaide 5001, Australia

S. Ait-Tahar and I. P. Grant

Mathematical Institute, Oxford University, 24-29 St. Giles, Oxford OX1 3LB, United Kingdom

P. H. Norrington

Department of Applied Mathematics and Theoretical Physics, The Queen's University of Belfast, Belfast BT7 1NN, Northern Ireland

(Received 2 October 1998)

Experimental benchmark results for the differential cross section and several spin asymmetries are presented for elastic electron scattering from Cs atoms at an energy of 3 eV. Comparison with predictions from several nonrelativistic, semirelativistic, and fully relativistic theoretical models emphasizes the need for the development of a numerical approach that accounts both for relativistic effects and for coupling between a large number of discrete and continuum target states. [S0031-9007(99)08422-7]

PACS numbers: 34.80.Dp

Electron scattering from alkali atoms has received considerable attention over the past two decades, theoretically as well as experimentally. In particular, spin-dependent angle-differential measurements of spin asymmetries for the light alkalis sodium [1,2] and lithium [3] provided important benchmarks, as the data allowed for a comprehensive test of newly developed theoretical methods. Ultimately, the very good agreement between experiment and predictions obtained from the “convergent-close-coupling” (CCC) approach [4] gave enormous confidence in the use of this theoretical method.

For the heaviest stable alkali atom, cesium, however, the current situation is much less clear. Experimentally, angle-differential work on this target has been scarce. Outstanding in this respect are the efforts of Gehenn and Reichert [5] who measured the shape of the elastic differential cross section (DCS) from 0.8 to 20 eV in the angular range between 30° and 150°. Klewer, Beerlage, and van der Wiel [6] measured the spin polarization of initially unpolarized electrons after scattering from unpolarized targets for energies of 13.5, 20, and 25 eV.

On the theoretical side, recent work includes the non-relativistic CCC calculation of Bartschat and Bray [7], a semirelativistic approach of Bartschat [8], and fully relativistic models of Thumm and Norcross [9] and of Ait-Tahar, Grant, and Norrington [10]. (References to earlier work can be found in these publications.) While the CCC model accounted for the coupling of approximately 40 discrete and continuum target states, it did not include any relativistic effects. The other methods, all based

on the *R*-matrix formulation of close-coupling theory, took into account only the coupling between the lowest five or eight discrete target states, but relativistic effects were included either perturbatively through the dominant terms of the Breit-Pauli Hamiltonian [8] or *ab initio* by using a formulation based upon the Dirac equation [9,10]. Only Ait-Tahar *et al.* [10] treated the interaction of all 56 electrons (55 in the target plus the projectile) explicitly, while the other approaches applied a model potential to simulate the effect of 54 core electrons. Although possibly less satisfactory from a fundamental point of view, such model potentials offer the advantage of accounting for effects like core polarization in a semiempirical way, thereby often improving upon the description of the target structure over an all-electron model with a limited number of configurations.

The problem of interest for the present paper, elastic electron scattering from cesium atoms, was analyzed 25 years ago in general terms by Burke and Mitchell [11] who, like Walker [12], also performed some calculations to illustrate the effects to be expected. Many of the parameters introduced in their paper, however, have never been determined experimentally, due to the need of preparing spin-polarized projectile and target beams before the collision and measuring the polarizations thereafter. It was not until 1995, for example, that the first results for the spin asymmetry functions discussed below were published [13], for incident electron energies of 7, 13.5, and 20 eV. At the time, no comparison with theoretical predictions was possible, since these “intermediate

energies,” between approximately 2 and 5 times the ionization threshold (3.9 eV), are very difficult to handle numerically. In the meantime, some comparisons have been made with these data, but either the theoretical method did not include relativistic effects [7] or it was at least questionable whether a low-energy approach was suitable for the collision energies of interest [10].

In this joint experimental and theoretical effort, therefore, we attempt to provide a highly accurate benchmark set of experimental data and compare them with theoretical predictions obtained from the most sophisticated currently available models. The chosen energy of 3 eV represents a compromise between experimental (beam control, count rates) and theoretical (expected validity of a low-energy close-coupling approach) feasibilities. Consequently, this is the first time that a comparison between experiment and theory is possible in a region where the presently available relativistic close-coupling theories might be sufficiently reliable.

Using parity conservation and time-reversal invariance of the interaction, Burke and Mitchell [11] found that six complex amplitudes are needed to completely describe the collision process. They also expressed various scattering parameters in terms of these amplitudes. In particular, the differential cross section for the scattering of spin-polarized beams is given by

$$\sigma = \sigma_0[1 + A_1(\mathbf{P}_a \cdot \hat{\mathbf{n}}) + A_2(\mathbf{P}_e \cdot \hat{\mathbf{n}}) - A_{nn}(\mathbf{P}_a \cdot \hat{\mathbf{n}})(\mathbf{P}_e \cdot \hat{\mathbf{n}})], \quad (1)$$

where σ_0 is the differential cross section for unpolarized beams, \mathbf{P}_a and \mathbf{P}_e are vectors describing the atomic and electron beam polarizations, respectively, and $\hat{\mathbf{n}}$ is the unit vector of the scattering plane.

The physical meaning of the spin asymmetries defined above can be summarized as follows: A_1 and A_2 correspond to “spin up–spin down” (with respect to the reaction plane) asymmetries in the DCS for scattering of unpolarized electrons from polarized atoms (A_1) or polarized electrons from unpolarized atoms (A_2), while A_{nn} represents an “antiparallel–parallel” asymmetry. In analogy to the nonrelativistic case, A_{nn} is

often called an “exchange asymmetry,” but we note that not only the relative orientation of the projectile and target spins is relevant but also their orientation with respect to the reaction plane [11]. Furthermore, A_2 is identical to the Sherman function, i.e., it also describes the left-right asymmetry in the differential cross section for scattering of spin-polarized electrons from unpolarized targets. Finally, as pointed out by Farago [14], nonvanishing values of A_1 require the simultaneous presence of spin-orbit and exchange effects, and hence this parameter is often called the “interference asymmetry.” Not surprisingly, attempts to measure nonzero A_1 values failed for the light sodium target [15] but were indeed successful using the heavier cesium target at the sufficiently low energy of 7 eV [13].

Experimentally, we determine these asymmetries by observing event yields for different combinations of projectile and target spin orientations. Specifically, we produce beam polarizations perpendicular to the reaction plane and measure four spin-dependent differential cross sections relative to each other by observing the count rates $N^{\uparrow\uparrow}$, $N^{\uparrow\downarrow}$, $N^{\downarrow\uparrow}$, and $N^{\downarrow\downarrow}$, where the first superscript indicates the target and the second indicates the projectile spin with respect to the scattering plane. From the accumulated background corrected rates we form raw asymmetries by building suitable combinations of spin-dependent settings from Eq. (1). We then obtain A_1 , A_2 , and A_{nn} by normalizing to unity polarizations with P_a , P_e , and $P_a \cdot P_e$, respectively. Unpolarized atomic beams are simulated by taking the average of $N^{\uparrow\uparrow}$ and $N^{\downarrow\uparrow}$ for electrons with spin “up” and of $N^{\uparrow\downarrow}$ and $N^{\downarrow\downarrow}$ for electrons with spin “down,” respectively, and similar averages are constructed to simulate an unpolarized electron beam.

The scheme of our experimental setup, described in detail in Ref. [13], is shown in Fig. 1. The polarized electron beam is produced by photoemission from a strained GaAs crystal [16] using light from a GaAlAs laser diode operating at a wavelength of 830 nm. A Pockels cell is used for generating either right or left circularly polarized light, leading to a transverse spin direction either parallel or antiparallel to $\hat{\mathbf{n}}$. Electron optical elements

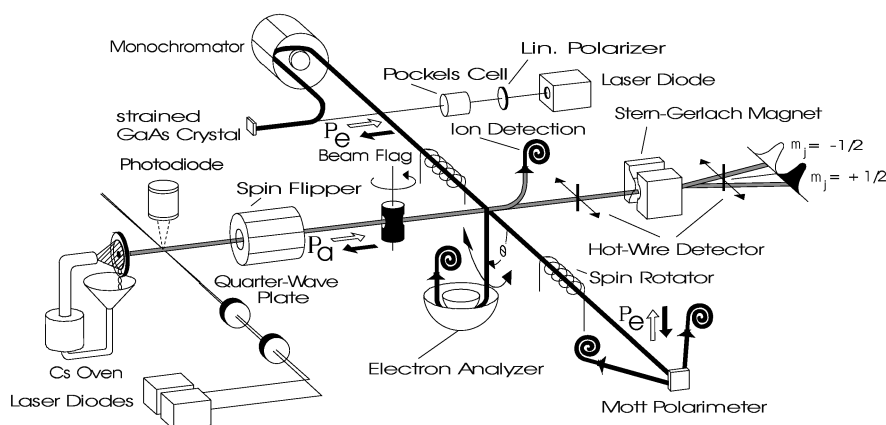


FIG. 1. Schematic setup of the experiment.

in front of and behind the collision region ensure a proper guiding of the electron beam with the main purpose of avoiding high background count rates. With the strained crystal we obtain currents of $0.5 \mu\text{A}$ in the scattering region and a polarization of $P_e = 0.65$, as measured with a retarding field Mott polarimeter. For the low-energy measurements, the 180° electrostatic monochromator with a central radius of 2.5 cm is set to provide an energy spread of $\Delta E = 150 \text{ meV}$ in the beam.

The spin-polarized atomic beam was also described previously (see Ref. [17]). It is produced from a recirculating Cs oven, which is reloadable under vacuum after 200 hours continuous operating time. For polarizing we use optical pumping with two laser diodes in single-mode operation, tuned to transitions from both hyperfine levels of the ground state. We obtain a polarization of $P_a = 0.9$, as measured with a Stern-Gerlach magnet, at an atomic beam density of $5 \times 10^9/\text{cm}^3$ in the scattering center. A spin flipper in front of the scattering chamber allows for reversal of the atomic beam polarization.

In the scattering chamber, the hemispherical electron energy analyzer is located below the plane of the two horizontal crossed beams and can be rotated around the atomic beam axis, from scattering angles of 40° to 140° . The analyzer has a central radius of 3.3 cm and is operated with a resolution of $\Delta E/E = 4.5\%$ to select the elastically scattered events. The five-element electron-optical lens system at the entrance to the analyzer defines the accepted phase space, as determined with an electron-optical simulation program. In the course of our investigations, we noticed that we could not always reproduce the shape of the DCS measured by Gehenn and Reichert [5]. This was traced back to the influence of background originating from electrons scattered by the atomic beam with a high rate into the forward direction. We eliminated this adverse effect by installing a collimator in the lens system, by increasing the distance of electron-optical elements from the scattering center, and by relying upon results of electron ray tracing to find settings with a favorable form of the accepted phase space.

An ion detector was installed to monitor the production of Cs^+ ions by scanning the projectile energy in the vicinity of the threshold at 3.9 eV. Hereby, we can observe the onset of ionization with an accuracy of $\pm 0.1 \text{ eV}$ which we use for calibration of the energy scale. In addition, comparing the observed spin asymmetry in the total ionization cross section with our earlier measurements [18] gives an easy and fast cross check on the correct spin settings, particularly on the collinearity of P_a and P_e . Furthermore, the spin settings are alternated in short time intervals to reduce systematic errors, and determinations of background rates are interspersed by shutting off the atomic beam.

Figure 2 shows our results at 3 eV incident energy for the differential cross section (normalized to theory at 90° scattering angle) and for the asymmetries A_{nm} , A_2 , and A_1 , all taken with an energy resolution of 150 meV

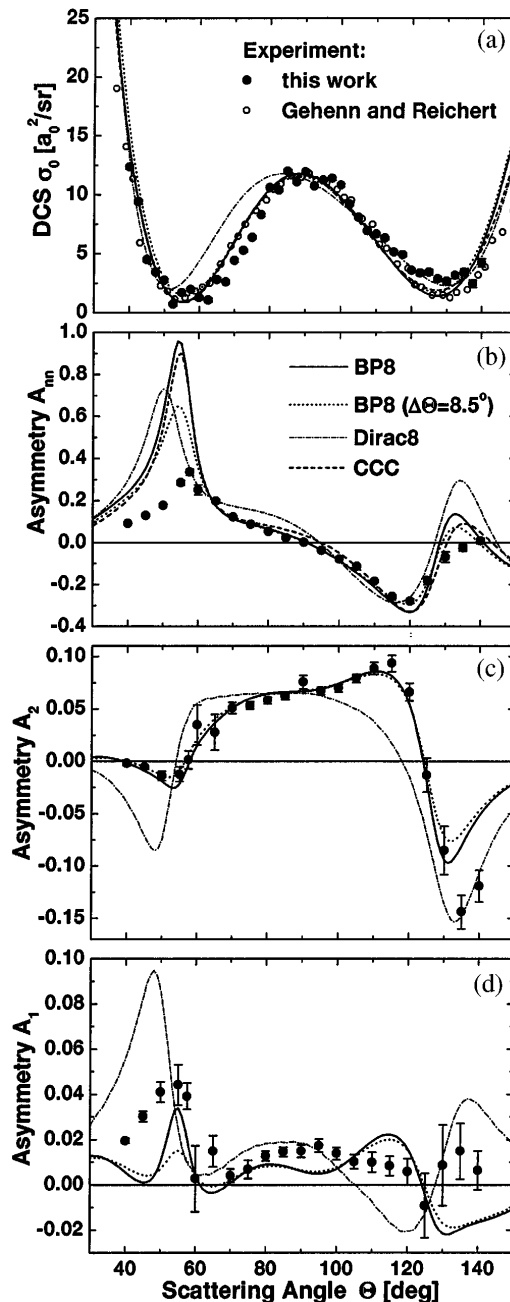


FIG. 2. Differential cross section σ_0 (a), normalized to the BP8 theory at a scattering angle of 90° , and spin asymmetries A_{nm} (b), A_2 (c), and A_1 (d) for elastic electron scattering from cesium atoms at an energy of 3 eV. The experimental results are compared with theoretical predictions described in the text. In order to compare the shapes of the DCS with the measurements, the CCC and Dirac8 results were multiplied by 0.82 and 1.12, respectively.

and angular resolution of 8.5° (FWHM). We compare the data with predictions from a semirelativistic 8-state Breit-Pauli R -matrix approach (BP8), a relativistic Dirac 8-state R -matrix model (Dirac8), and a nonrelativistic CCC calculation. To illustrate the effect of finite detector openings, the Breit-Pauli results are also shown after convolution with the experimental angular resolution.

For the DCS (Fig. 2a), very satisfactory agreement is seen among the experimental and theoretical results for the shape as a function of the scattering angle, except for some deviations exhibited in the Dirac results which predict the first minimum at smaller scattering angles and not as deep as the other models. In order to compare the shapes, the experimental results were normalized to the BP8 theory at $\theta = 90^\circ$, and the CCC and Dirac8 results were multiplied by 0.82 and 1.12, respectively. These findings are consistent with several important, though preliminary, conclusions, namely: (i) Relativistic effects have only a small influence on the theoretical DCS results; (ii) at least for the relative DCS, the BP8 calculation seems to have converged sufficiently with respect to the number of states included; (iii) the differences between the BP8 and Dirac8 results are probably due mostly to the absence of core polarization in the latter [10].

These conclusions are further supported by investigating the results for the spin asymmetry A_{nn} (Fig. 2b), for which experiment and theory agree quite nicely in the angular range from $\theta = 55^\circ$ to 125° . Again, CCC and BP8 agree very well with each other, while the Dirac results exhibit small but significant deviations from the other theoretical predictions and also from experiment. Near the forward ($\theta \approx 55^\circ$) and the backward ($\theta \approx 130^\circ$) cross section minima, the theories predict pronounced structures with asymmetry values up to +1 at about 55° . The experimental data, however, do not reflect this behavior but instead show a tendency towards diminishing asymmetries for small and large scattering angles. Although accounting for the experimental angular resolution reduces the asymmetry predicted by the BP8 model considerably, the effect of the convolution is not sufficient to state satisfactory agreement between theory and experiment. One might speculate that minute contaminations in the beam reduce the measured asymmetry, particularly visible near cross section minima. Through careful checks of the experimental procedure, we can exclude a detectable influence of dimers (Cs_2) in the beam on the measured asymmetry.

Our data for the spin asymmetries A_2 (Fig. 2c) and A_1 (Fig. 2d) are compared only with the two relativistic predictions, since the nonrelativistic result is exactly zero. Nearly perfect agreement exists between experiment and the Breit-Pauli results for A_2 ; only the data points for the two largest angles lie significantly below the prediction. The results of the Dirac treatment, however, deviate considerably from the Breit-Pauli curve and thus disagree with experiment, especially in the angular ranges from 30° to 50° and from 100° to 130° .

As one might expect, the spin asymmetry A_1 is the most sensitive parameter with respect to the details of the theoretical model, as it is small to begin with and is affected by both exchange and relativistic effects. Here the two theoretical treatments predict distinctly different results. Both show a sharp peak of the asymmetry in the forward direction, but of considerably different size and location,

and structure in the backward scattering region, although with opposing angular dependence and even different signs of the asymmetry. The measurements show reasonable agreement with the predictions in the limited angular range from 60° to 105° , but deviate below and above this range. Note that in this case the experimental data near the forward direction lie significantly above the convoluted BP8 predictions. Since (i) convergence in one observable does *not* necessarily imply convergence in another and (ii) convergence may be more difficult to achieve in such a sensitive parameter, one might expect that a CCC-type treatment of this collision, even at such low energies, will improve the agreement between theory and experiment for the spin asymmetry A_1 .

In conclusion, using highly polarized beams of electrons and cesium atoms, we have obtained statistically precise data for several spin asymmetries in low-energy e -Cs scattering, with absolute uncertainties $\delta A < \pm 0.005$ for most angles in the angular range from 40° to 140° . The present data at 3 eV are expected to provide a set of benchmarks needed for further theoretical developments, particularly with respect to a relativistic CCC-type approach. Further work on this system will include measurements at higher energies (up to 10 eV), where the coupling to the target continuum states should become more important in theoretical treatments, and the extension to inelastic and superelastic collisions involving the $6s \leftrightarrow 6p$ transition.

This work was supported, in part, by the Deutsche Forschungsgemeinschaft through SFB 216 (G. B., W. R., B. R., M. T.), by the United States National Science Foundation under Grant No. PHY-9605124 (K. B.), by the Australian Research Council (I. B.), and by the United Kingdom Science and Engineering Research Council (S. A. T.).

-
- [1] S. R. Lorentz *et al.*, Phys. Rev. Lett. **67**, 3761 (1991).
 - [2] J. J. McClelland *et al.*, Phys. Rev. A **46**, 6079 (1992).
 - [3] G. Baum *et al.*, Phys. Rev. Lett. **57**, 1855 (1986).
 - [4] I. Bray, Phys. Rev. A **49**, 1066 (1994).
 - [5] W. Gehenn and E. Reichert, J. Phys. B **10**, 3105 (1977).
 - [6] M. Klewer, M. J. M. Beerlage, and M. J. van der Wiel, J. Phys. B **12**, L525 (1979).
 - [7] K. Bartschat and I. Bray, Phys. Rev. A **54**, 1723 (1996).
 - [8] K. Bartschat, J. Phys. B **26**, 3695 (1993).
 - [9] U. Thumm and D. W. Norcross, Phys. Rev. Lett. **67**, 3495 (1991); Phys. Rev. A **45**, 6349 (1992); **47**, 305 (1993).
 - [10] S. Ait-Tahar, I. P. Grant, and P. H. Norrington, Phys. Rev. Lett. **79**, 2955 (1997).
 - [11] P. G. Burke and J. F. B. Mitchell, J. Phys. B **7**, 214 (1974).
 - [12] D. W. Walker, J. Phys. B **7**, L489 (1974).
 - [13] B. Leuer *et al.*, Z. Phys. D **33**, 39 (1995).
 - [14] P. S. Farago, J. Phys. B **7**, L28 (1974).
 - [15] J. J. McClelland *et al.*, J. Phys. B **23**, L21 (1990).
 - [16] R. Prepost and T. Maruyama, Annu. Rev. Nucl. Part. Sci. **45**, 411 (1995).
 - [17] G. Baum *et al.*, Z. Phys. D **22**, 431 (1991).
 - [18] G. Baum *et al.*, J. Phys. B **26**, 331 (1993).